Raman Spectroscopic Studies of Silicotitanates

Yali Su* and Mari Lou Balmer

Materials Resources and Environmental Molecular Science Laboratory, Pacific Northwest National Laboratory, Richland, Washington 99352

Bruce C. Bunker

Sandia National Laboratories, Albuquerque, New Mexico 87185

Received: May 22, 2000

Silicotitanates are nanoporous materials that have been used as selective ion exchangers for removing cesium from waste streams and catalysts for promoting oxidation and hydroxylation reactions. The local bonding configurations and network charge distribution are known to influence the selectivity and reactivity of these compounds. We have synthesized a group of new silicotitanates using sol−gel and solid-state techniques. Raman spectroscopy has been used to systematically examine the vibrational behavior of these compounds. By correlating the variations of Raman spectra with titanium coordinations of these compounds, the relationship between Raman shifts and the local bonding configurations around silicon and titanium is proposed.

Introduction

Silicotitanate materials represent excellent ion exchangers for selective removal of radioactive Cs and Sr from tank waste.[1] Silicotitanates also exhibit exceptional catalytic activity and selectivity for oxidation reactions. [2,3] Research is under way to try to relate these interesting properties to the local bonding configurations of the silicon and titanium sites that are present in such materials. Previous characterization studies of many single-crystal silicotitanates provide detailed structural information.[4−15] However, due to the unavailability of single-crystal silicotitanates, local bonding configurations of Ti and Si in some silicotitanate compounds are not well understood. Recently, Bunker and Balmer developed a methodology for predicting the Ti coordination in silicotitanates.[16] Systematic ^{29}Si NMR investigations have also been conducted to elucidate the relationship between chemical shifts and number of titanium polyhedral coordinations for a given silicon tetrahedron.[17] The results clearly indicate that systematic downfield chemical shifts occur with an increasing number of titanium polyhedra coordinating a given silicon tetrahedron. This interesting discovery stimulated our investigation on the Ti local coordination by Raman spectroscopy, which is capable of providing a different perspective of the local bonding configurations. Raman spectroscopy is an effective structural tool capable of discriminating or "fingerprinting" different local bonding configurations.

While Si^{4+} is always tetrahedrally coordinated by oxygen anions, Ti^{4+} can occupy sites coordinated to 4, 5, or 6 oxygens (TiO_4, TiO_5, TiO_6). Such a variation in titanium coordination often leads to unusual changes in physical properties of silicotitanates. In previous studies where Raman spectroscopy was used to investigate the structure of silicates, Ti-bearing silicate glasses, and minerals, TiO_2 (rutile) and TiO_2 (anatase) were selected as reference crystals for Ti in 6-fold coordination.[18−20] The observed Raman peaks at 600−650 cm^{-1} were attributed to the Ti−O stretching vibrations of TiO_6 octahedra.[18−20] Raman bands in the 750−900 cm^{-1} region were assigned to Ti−O stretching vibrations of TiO_4 tetrahedra in titanates.[18−20] This is consistent with other observations that show in general the metal−oxygen bond of a lower coordination unit is stronger, and thus produces a Raman peak at higher frequency than that of a higher coordination unit.[20] Compounds with TiO_5 coordination such as fresnoite contain a short apical Ti−O bond with a stronger Ti−O bond strength compared to that of TiO_4 and TiO_6. Consequently, Raman bands at higher frequencies (800−950 cm^{-1}) are assigned to the Ti−O stretch in TiO_5. [21−24] However, Raman studies of some titanates and silicotitanates with TiO_6 coordination show prominent bands ranging from 720 to 970 cm^{-1}. For example, ETS-10 shows a prominent band at 723 cm^{-1} which was assigned to the Ti−O stretch in TiO_6 coordination.[25] In addition, $Na_2Ti_3O_7$, $Na_2Ti_6O_{13}$, and $BaTi_4O_9$ exhibit Raman bands above 850 cm^{-1} [18] and $Cs_2TiSi_6O_{15}$, $BaTiSi_3O_9$, and $K_2TiSi_3O_9$ (see Figure 6 in later sections) have prominent Raman bands above 930 cm^{-1}. Furthermore, a band at 960 cm^{-1} was found in some titanium-substituted silicates with TiO_4 coordination. The assignment of these abnormally high-frequency bands is a matter of debate and, so far, the Raman spectra of silicotitanates have been interpreted in various and sometimes contradictory ways.[26−30]

The objective of this study is to obtain a more complete understanding of the vibrational modes observed for silicotitanates. Our focus is to use Raman spectroscopy to systematically investigate a series of silicotitanates with different titanium coordinations and to obtain the relationship between Raman shifts and coordination of titanium in these compounds.

Experimental Section

Silicotitanate samples were synthesized by a variety of techniques. $Na_2TiSi_4O_{11}$, $CsTiSi_2O_{6.5}$, $Na_2TiSi_2O_7$, and Na_2TiSiO_5 were made via a sol−gel synthesis route. For sol−gel synthesis, mixtures of tetraethyl orthosilicate (TEOS) and titanium isopropoxide (TIP) were hydrolyzed using a mixture of alkali hydroxide, water, and ethanol. After gelation, additional water was added to break up the gel, and the liquid was stirred and aged overnight. The mixture was slowly dried, then calcined

* Corresponding author. Fax: (509) 376-5106. E-mail: ya.su@pnl.gov.

10.1021/jp0018807 CCC: $19.00
Published on Web 07/28/2000

and heat-treated at desired temperatures. Heat-treatment temperatures and times varied on the basis of optimum synthesis conditions for the compound of interest. $Na_2TiSiO_4O_{11}$ formed after melting (at 1035 °C), grinding, and then heat treating to 800 °C for 12 h. Similarly, $Na_2TiSi_2O_7$ crystallized after melting at 985 °C, grinding, and then heat treating to 820 °C for 14 h. $CsTiSi_2O_{6.5}$ and Na_2TiSiO_5 formed directly after heat treatment to 800 °C for 1 h and 900 °C for 12 h, respectively.

$K_2TiSi_3O_9$, $Na_2Ti_2Si_2O_9$, and $Ba_2TiSi_2O_8$ (fresnoite) were synthesized from mixtures of SiO_2, TiO_2, K_2CO_3, Na_2CO_3, and $BaCO_3$. The powders were mixed using a mortar and pestle and subsequently heat-treated. Several cycles of grinding and heat treatment were necessary to form phase-pure compounds. Crystalline $K_2TiSi_3O_9$ and $Na_2Ti_2Si_2O_9$ formed after heat-treating powders to 1000 °C for 12 h and 900 °C for 24 h, respectively. $Ba_2TiSi_2O_8$ (fresnoite) crystallized after melting at 1200 °C and cooling to 900 °C for 24 h. The addition of $CsVO_3$ flux was necessary to synthesize $Cs_2TiSi_6O_{15}$. In this case, the component oxides were mixed and melted, ground with flux, and then heat-treated at 790 °C for at least 50 h. The mineral forms of $CaTiSiO_5$ (sphene or titanate, Wards Geology, Rochester, NY), $BaTiSi_3O_9$ (benitoite, supplied by the National Museum of Natural History, Smithsonian Institution, benitoite-California-87424), and $Na_2TiSi_4O_{11}$ (Narsarsukite, supplied by the National Museum of Natural History, Smithsonian Institution, narsarsukite-Greenland-138948) were used. ETS-10 and ETS-4 were obtained from Engelhard Corp. X-ray diffraction was used to analyze all mineral and synthetic samples for phase content and purity.

Raman spectra were collected using a Spex Triple Raman Spectrometer (Industries model 1977) with the 488 nm line of a Spectra Physics model 164 Ar^+ ion laser for excitation. The power at the sample was on the order of 300 mW. A LN/CCD detector (Princeton Instruments) was used with a typical exposure time of 100 s and a slit width of 100 μm. Raman spectra were obtained at 180° scattering geometry on pellets of pressed powder. The Raman peak positions were measured on the basis of the reference of the known bands of anatase with an accuracy within ± 2 cm^{-1}. Spectral analysis was performed using commercial software (Galactic Industries Grams/32).

Results and Discussion

Several typical bond lengths and local geometries of Si and Ti are illustrated in Figure 1. In general, there are three kinds of connections observed for TiO_6, TiO_5, and SiO_4 polyhedra. They are TiO_6−TiO_6 chains, TiO_5−TiO_5 chains, and SiO_4−TiO_6 chains. The Ti−O lengths in TiO_6 are typically equal for all Ti−O bonds and range from 1.9 to 2.1 Å, whereas the Ti−O bond lengths in TiO_5 compounds vary significantly. In the case of TiO_5, the apical oxygen is strongly bonded to titanium, forming what can be considered as a double Ti═O bond. This oxygen is not considered to be bonded to other titaniums in the structure. Bond lengths for the apical bond are approximately 1.7 Å. The opposing Ti···O bond is typically elongated with lengths near 2.3 Å. The bond length of tetrahedral bridging Si−O bonds is around 1.6 Å, as indicated in Figure 1. On the basis of bond length and strength considerations, the Raman vibrational frequencies are expected to decrease as follows: ν(Si−O$^-$) > ν(Ti═O) > ν(Ti−O). Here the Si−O$^-$ refers to the Si−O nonbridging oxygen bond. The Raman frequency of Si−O−Si bridging oxygen bonds will be below 600 cm^{-1} and will be discussed later.

Among twelve silicotitanates studied (see Table 1), seven compounds—$Cs_2TiSi_6O_{15}$, $BaTiSi_3O_9$, ETS-10, $Na_2TiSi_4O_{11}$, $CaTiSiO_5$, $K_2TiSi_3O_9$, and $Na_2Ti_2Si_2O_9$—contain TiO_6 polyhedra; two compounds—Na_2TiSiO_5 and $Ba_2TiSi_2O_8$—contain TiO_5 polyhedra; and three compounds—$CsTiSi_2O_{6.5}$, ETS-4, and $Na_2TiSi_2O_7$ —have unknown structures. The compositions of unknown compounds all fall within regions of the phase diagram where TiO_5 or TiO_6 are preferred, as shown in Figure 2.[16] These different titanium coordinations and local network structures are expected to have unique Raman shifts. In the following sections, compounds are grouped and discussed on the basis of similarities in the short- and long-range titanium coordination geometries.

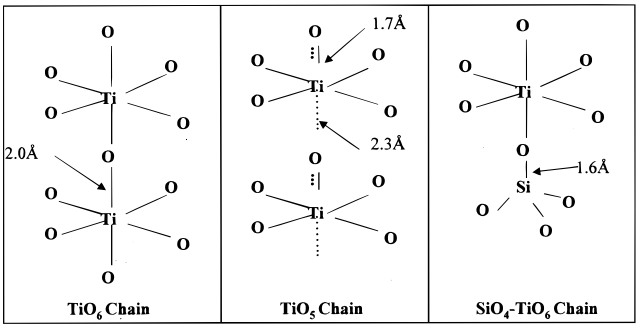

Figure 1. Ti and Si coordination in silicotitanates.

I. ETS-10, $Na_2TiSi_4O_{11}$, and $CaTiSiO_5$. ETS-10 is a microporous crystalline silicotitanate, and its approximate chemical formula is $M_{16}Ti_8Si_{39}O_{104}$, where M is sodium or potassium.[31] ETS-10 and $Na_2TiSi_4O_{11}$ both have TiO_6 octahedra that are joined at the vertexes to form chains of titania polyhedra. In ETS-10, corner-sharing SiO_4 tetrahedra and TiO_6 octahedra are linked through bridging oxygen atoms.[6] TiO_6 octahedra are coordinated by four silicon and two titanium atoms. In $Na_2TiSi_4O_{11}$ chains of titanium octahedra joined by opposite vertexes are bonded to $[Si_4O_{10}]$ chains made up of four-membered rings of SiO_4 tetrahedra.[7] The crystal structures of these two compounds are illustrated in Figure 3. Figure 4 shows the Raman spectra of ETS-10 and $Na_2TiSi_4O_{11}$. The most intense peak was found to be at approximately 750 cm^{-1} in these compounds, i.e., 729 cm^{-1} for ETS-10, and 764 cm^{-1} for $Na_2TiSi_4O_{11}$, respectively. The Raman spectra from ETS-10 is consistent with those reported by Hong et al.[25] In their study the most prominent band was found to be at 723 cm^{-1}, and was assigned to the Ti−O stretching vibrations of TiO_6 units.[25] In addition, a Raman band at 764 cm^{-1} has been reported in a new synthetic nenadkevichite which exhibits the same kind of TiO_6 chain structure.[32] We attribute the strong band at ∼750 cm^{-1} in the Raman spectra of ETS-10, $Na_2TiSi_4O_{11}$, and nenadkevichite to the Ti−O−Ti stretch in corner-shared TiO_6 chains. This characteristic band can be regarded as a useful probe for characterization of silicotitanates with titanium in six-coordinate, corner-shared TiO_6 chains.

The crystal structure of $CaTiSiO_5$ consists of kinked chains of corner-sharing TiO_6 octahedra cross-linked by silicon tetrahedra. [8,9] The silicon tetrahedra share oxygen atoms with four separate Ti octahedra in three separate chains, and the oxygen atoms are shared by two network-forming cations. The titanium is in a distorted octahedral coordination and is displaced toward one apical oxygen. The octahedra form linear chains linked by two opposite apexes. Figure 5 shows the Raman spectrum of $CaTiSiO_5$. Instead of having one prominent band at ∼750 cm^{-1} (as in ETS-10 and $Na_2TiSi_4O_{11}$), $CaTiSiO_5$ has a prominent band at 611 cm^{-1}, several medium-strength bands at 253, 324, 468, and 549 cm^{-1}, and weak bands at 865, 913, and 1005 cm^{-1}. Similar to $Na_2TiSi_4O_{11}$, $CaTiSiO_5$ has corner-linked TiO_6.

TABLE 1: Twelve Compounds with the Structure Data

compounds	Ti coordinates	structure units	Ti−O bond lengths (Å)	Si−O bond lengths (Å)
ETS-10	6	corner-shared TiO_6 chains	1.901, 1.907	1.575−1.585
$Na_2TiSi_4O_{11}$	6	corner-shared TiO_6 chains	1.904, 1.966, 2.070	1.601−1.639
$Cs_2TiSi_6O_{15}$	6	TiO_6−SiO_4 chains	1.938, 1.939	1.580−1.638
$K_2TiSi_3O_9$	6	TiO_6−SiO_4 chains	2.004	1.561−1.625
$BaTiSi_3O_9$	6	TiO_6−SiO_4 chains	1.943	1.605−1.648
$CaTiSiO_5$	6	corner-shared TiO_6 chains	*1.766*, 1,973, 1.984, 1.991, 2.014, 2.025	1.646
$Na_2Ti_2Si_2O_9$	6	edge-shared TiO_6 chains	1.85, 1.88, 1.94, 1.95, 2.16	1.60−1.69
$Ba_2TiSi_2O_8$	5	TiO_5, one short Ti−O bond	*1.66*, 2.00 (×4)	1.65
Na_2TiSiO_5	5	TiO_5, one short Ti−O bond	*1.695*, 1.990 (×4)	1.636
$CsTiSi_2O_{6.5}$	5?	?	?	
ETS-4	6?	?	?	
$Na_2TiSi_2O_7$	6?	?	?	

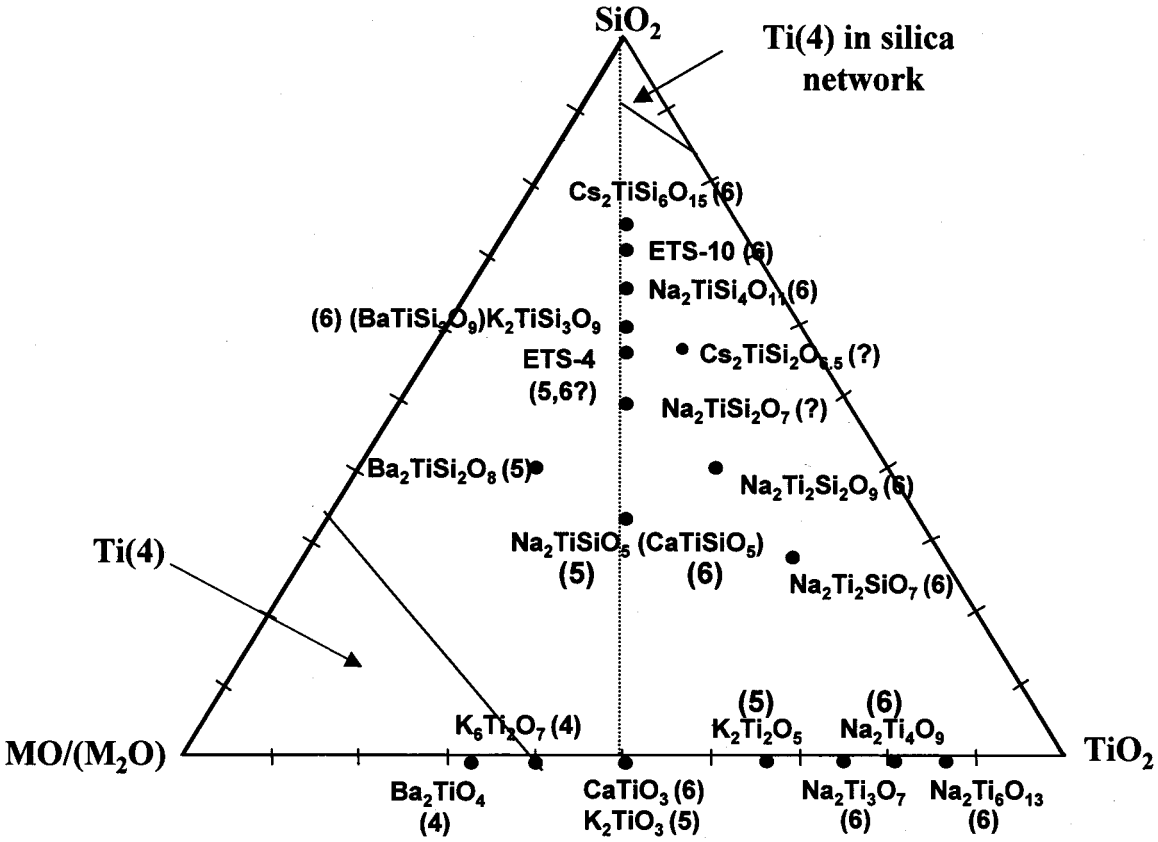

Figure 2. Compounds in silicotitanate phase diagrams. Titanium coordination numbers are given in (). Compositions are in mole oxide.

However, Ti in $CaTiSiO_5$ is in a distorted octahedral coordination. One of the Ti−O bond lengths is as short as 1.77 Å. As shown in Section IV, this short Ti−O bond in the isolated TiO_5 structure exhibits a strong peak at approximately 850 cm^{-1}, similar to that observed for $CaTiSiO_5$. However, for $CaTiSiO_5$ the intensity of the 850 cm^{-1} band is much lower than that typically observed for compounds with isolated TiO_5 polyhedra. This probably is due to the fact that Ti−O vibrational averaging occurs along the TiO_6 chains in which the short bond in $CaTiSiO_5$ is included. The strong asymmetric and broad peak at 611 cm^{-1} may indicate a combination of Ti−O vibrational averaging and Si−O−Si symmetric vibrations.

As indicated in the Introduction, anatase and rutile are often used as reference crystals for Ti in 6-fold coordination, and the Raman band at 600−650 cm^{-1} has been assigned to the Ti−O stretching vibration of TiO_6.[18−20] This seems to contradict the assertion that the band at 750 cm^{-1} is characteristic of TiO_6 chains as we discussed above. In fact, both anatase and rutile contain edge-shared TiO_6 chains and three-coordinate oxygen. In contrast, ETS-10 and $Na_2TiSi_4O_{11}$ contain corner-shared TiO_6 chains and two-coordinate oxygens. Therefore, it is expected that anatase and rutile would have unique Raman shifts as compared to silicotitanates with corner-shared Ti octahedra with 2-coordinate oxygens and their Raman shifts should not be used as a standard for Ti−O stretching for all silicotitanates containing octahedral titanium.

II. $Cs_2TiSi_6O_{15}$, $BaTiSi_3O_9$ (benitoite), and $K_2TiSi_3O_9$. In $Cs_2TiSi_6O_{15}$, $BaTiSi_3O_9$, and $K_2TiSi_3O_9$, titanium octahedra are isolated (i.e., no Ti−O−Ti bonds) in a silicate network, therefore there are only Ti−O−Si and Si−O−Si linkages. The structural building units of $Cs_2TiSi_6O_{15}$ are a titanium-centered octahedron, a Si_2O_7 group containing Si(1), and two further silicon-centered tetrahedra containing Si(2) and Si(3). The polyhedra are connected by corner-sharing of all vertexes to form an open framework. The TiO_6 octahedra are indirectly linked to one another via two intervening SiO_4 tetrahedra, as shown in Figure

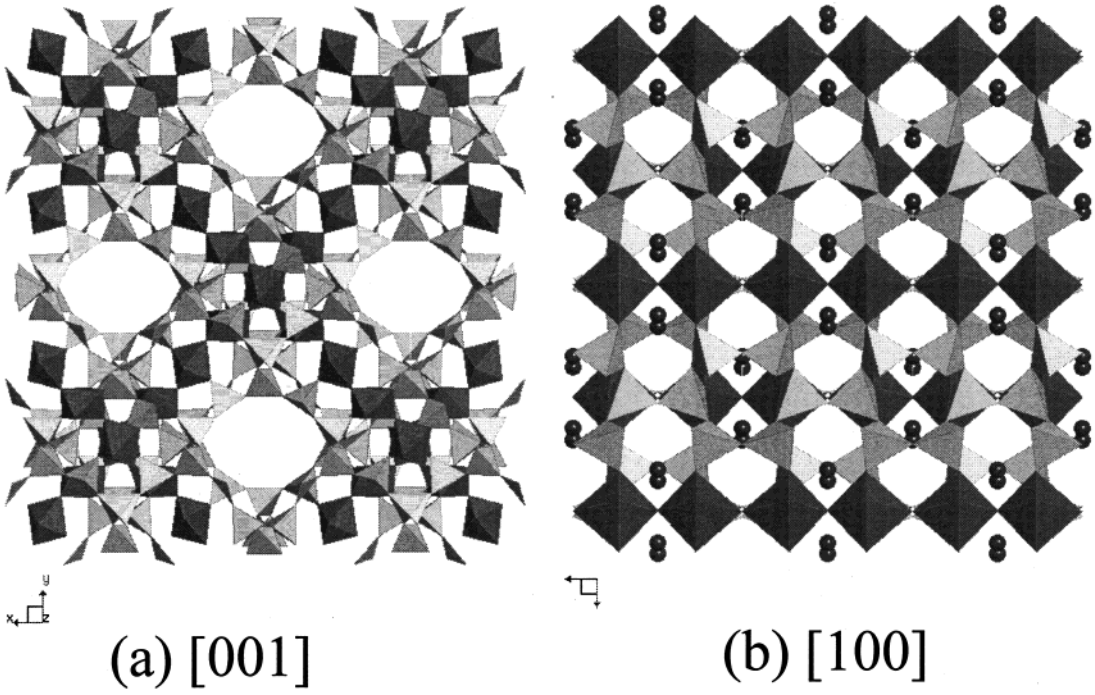

Figure 3. (a) ETS-10 and (b) $Na_2TiSi_4O_{11}$ crystal structure viewed from [001] and [100]. It is in TiO_6 coordination. The compounds contain corner-shared Ti−O−Ti chains.

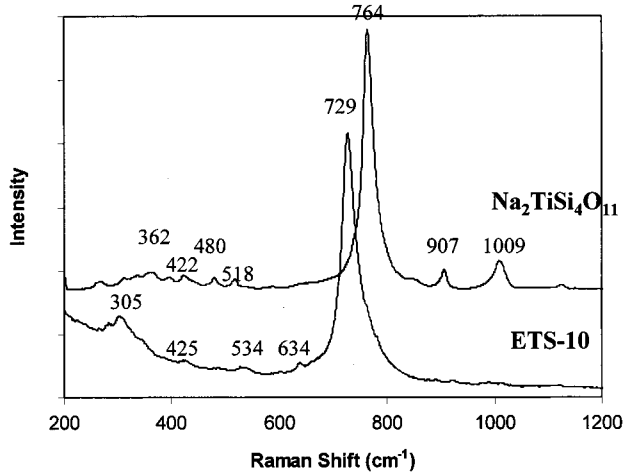

Figure 4. Raman spectra of ETS-10, $Na_2TiSi_4O_{11}$, and $Na_2TiSi_2O_7$.

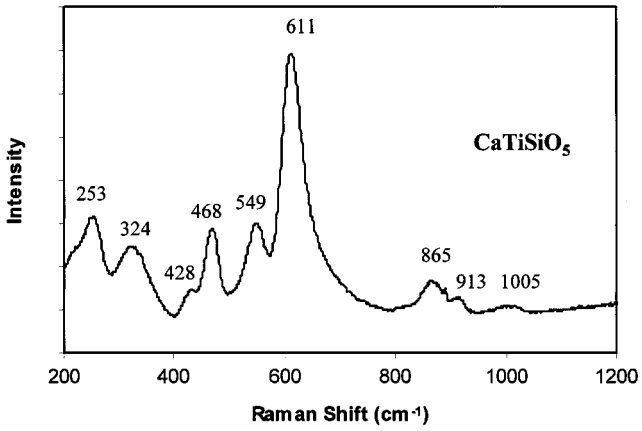

Figure 5. Raman spectrum of $CaTiSiO_5$.

6a.[4] There are three unique Si sites with twelve unique Si−O bond lengths ranging from 1.58 to 1.64 Å. In comparison, all Ti−O bond lengths are 1.94 Å. $BaTiSi_3O_9$ (benitoite) contains isolated octahedral titanium which is connected to Si_3O_9 rings as shown in Figure 6b.[5] The bond lengths of Ti−O are all 1.94 Å, and are 1.63, 1.648, and 1.605 Å for Si−O. The $K_2TiSi_3O_9$ structure can be envisioned as consisting of layers of $[Si_3O_9]$ rings that are linked by octahedrally coordinated Ti into a three-dimensional framework, as shown in Figure 6c.[33] Potassium occupies nine-coordinated cage sites that are staggered between neighboring layers of $[Si_3O_9]$ rings. There are two symmetrically distinct oxygens: O(1) is bonded to two Si, and O(2) is bonded to one Si and one Ti. All Ti−O bond lengths are 2.004 Å and Si−O bond lengths are 1.561 Å (all Si−O−Ti), and 1.614 to 1.625 Å (Si−O−Si). Figure 7shows the Raman spectra of $Cs_2TiSi_6O_{15}$, $BaTiSi_3O_9$, and $K_2TiSi_3O_9$. Although in all three cases titanium is in TiO_6 coordination, there are no strong Raman peaks near 750 cm^{-1} (characteristic of the Ti−O−Ti stretch in corner-shared TiO_6 chains) as discussed in the previous section. Instead, each compound exhibits very strong peaks in the range of 930 to 980 cm^{-1}, and medium to strong peaks in the range of 515 to 570 cm^{-1}. For example, benitoite ($BaTiSi_3O_9$) exhibits two Raman bands at 930 and 943 cm^{-1}, which are consistent with the reported bands at 926 and 938 cm^{-1} for benitoite.[26,34] These results can be understood from the TiO_6 local structural configuration. SiO_4 units connect to TiO_6, forming $O_3Si-O-Ti$ units. The O−Ti bond in these units, which is considerably longer than Si−O bond in Si−O−Si linkages, can be compared to a nonbridging bond, $Si-O^-$. The strong bands at 930−980 cm^{-1} can be assigned to the $[O_3Si-O]^{\delta-}-[TiO_5]^{\delta+}$ stretch, similar to the O_3Si-O^- (one nonbridging oxygen) stretch in alkaline silicate glass.[35] Compared to the Raman shifts observed in silicate glass, the Raman peaks in the range of 400∼600 cm^{-1} and below 400 cm^{-1} can be assigned to the Si−O−Si symmetric stretch vibrations and the bending motions of the Si−O−Si and Si−O−Ti linkages, respectively.[35] Isolation of the TiO_6 octahedra by SiO_4 tetrahedra in these three compounds results in the elimination of the Raman peak at 750 cm^{-1} that is attributed to the Ti−O−Ti stretch in corner-shared TiO_6 chains.

A prominent band in the region of 930−980 cm^{-1} (here we refer to "960 cm^{-1}") has also been observed in silicates and

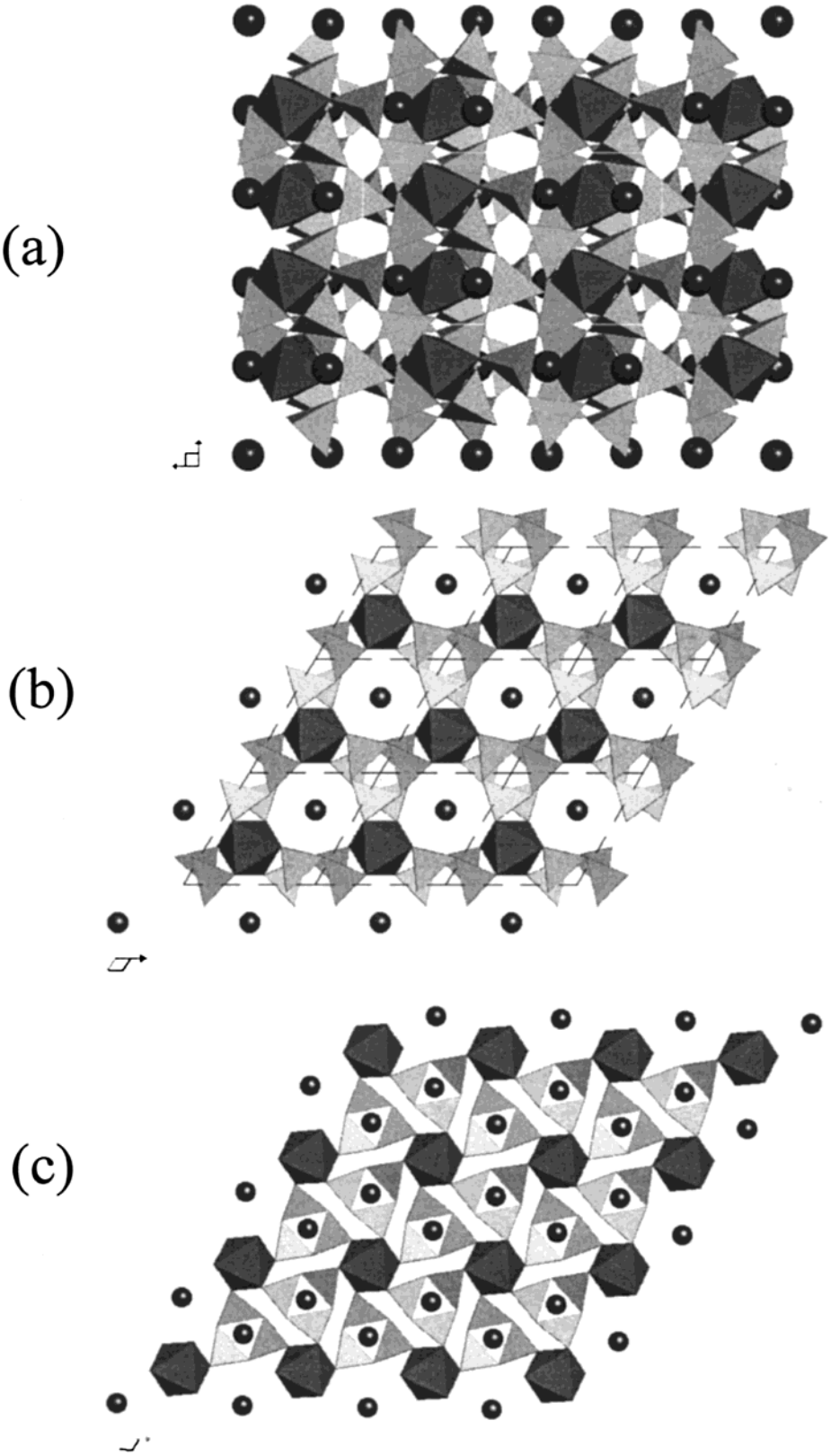

Figure 6. (a) $Cs_2TiSi_6O_{15}$, (b) $BaTiSiO_3$, and (c) $K_2TiSi_3O_9$ crystal structure viewed from [001]. Ti is in TiO_6 coordination. The compounds contain Si−O−Si, Ti−O−Si linkages, but no Ti−O−Ti chains.

zeolites.[27−29] However, the assignment of this band has been a matter of debate. Because the intensity of the "960 cm^{-1}" band increases with titanium substitution into a silicalite framework in titanium-substituted silicates, it has been regarded as an indication for the presence of titanium in the framework.[30] However, the "960 cm^{-1}" band is also observed in vanadium-substituted silicates and silicate glasses. Therefore, this band was suggested to be due to vibrations involved with silica rather than titanium.[29] Similar to the study compounds ($Cs_2TiSi_6O_{15}$, $BaTiSi_3O_9$, and $K_2TiSi_3O_9$), Ti- and V-substituted silicates with Si−O−Ti or Si−O−V linkages are expected to have a short Si−O bond (compared to O−Ti and O−V bonds) which results in a band near 960 cm^{-1}. A detailed review of silicate Raman spectra shows that vibrations arise in the 800−1200 cm^{-1} region

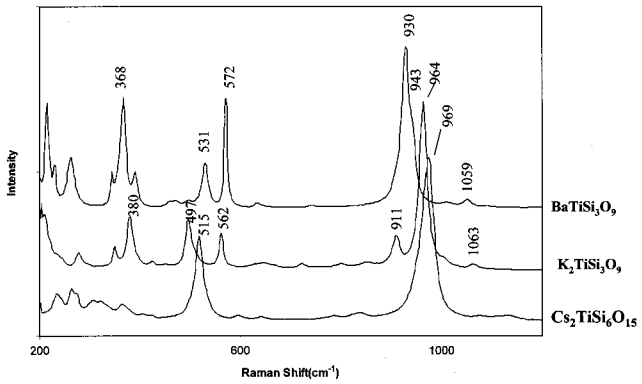

Figure 7. Raman spectra of $Cs_2TiSi_6O_{15}$, $BaTiSiO_3$, and $K_2TiSi_3O_9$.

when modifier cations are introduced into silicate materials. [35] In the high-frequency region (800−1200 cm^{-1}), Raman bands are assigned to the symmetric silicon−oxygen stretching motions of silicate units with one, two, three, or four nonbridging oxygens. These bands give rise to polarized bands at ∼1050, 950, 900, and 850 cm^{-1} respectively. According to this assignment, the "960 cm^{-1}" band which was observed in titanium-substituted zeolites was assigned to the vibration of "two nonbridging oxygens".[29] However, there are no nonbridging oxygens similar to these silicate networks in $Cs_2TiSi_6O_{15}$, $BaTiSi_3O_9$, and $K_2TiSi_3O_9$. Therefore, one cannot simply correlate the "960 cm^{-1}" bands in silicotitanates to vibrations only involved with silica. Rather, this vibration can be more generally attributed to a Si−O−Ti stretch. As we pointed out earlier in $Cs_2TiSi_6O_{15}$, $BaTiSi_3O_9$, and $K_2TiSi_3O_9$, SiO_4 units connect to TiO_6, forming $O_3Si-O-Ti$ units where the Si−O bond is short, and the O−Ti bond can be compared to a nonbridging bond. Thus, we assign the "960 cm^{-1}" band to $[O_3Si-O]^{\delta-}-[TiO_5]^{\delta+}$.

III. $Na_2Ti_2Si_2O_9$ (lorenzenite). In lorenzenite, the titanium coordination geometry is octahedral and the silicon tetrahedra form pyroxene-type (Si_2O_6) chains, where two of the oxygen atoms in each tetrahedron are bonded to silicon. One of the two remaining oxygen atoms in the silicon tetrahedron is three-coordinate and bonded to two titanium atoms, while the other is bonded to one titanium atom.[10,11] The TiO_6 polyhedra in $Na_2Ti_2Si_2O_9$ form distorted chains with Ti−O bond lengths ranging from 1.85 to 2.16 Å. The TiO_6 polyhedra share an edge with neighboring polyhedra and form zigzag TiO_6 polyhedra chains (see Figure 8). Pairs of TiO_6 chains are bonded through an apical Ti−O−Ti bond, similar to corner-shared Ti−O−Ti chains. The $Na_2Ti_2Si_2O_9$ sample used in this study had a minor impurity (approximately 4%) of $Na_2Ti_6O_{13}$ phase. To differentiate between Raman peaks that result from the $Na_2Ti_6O_{13}$ and $Na_2Ti_2Si_2O_9$, the Raman spectrum of pure $Na_2Ti_6O_{13}$ was obtained. Peaks due to $Na_2Ti_6O_{13}$ were then subtracted from the spectra of mixed $Na_2Ti_2Si_2O_9$ and $Na_2Ti_6O_{13}$ to yield a spectrum that represents the "pure" $Na_2Ti_2Si_2O_9$ (Figure 9a). The "pure" $Na_2Ti_2Si_2O_9$ spectrum exhibits relatively strong bands at 637, 704, 274, 305, 451, 486, and 538 cm^{-1}, and some weak bands in the high wavenumber region (above 800 cm^{-1}).

Interpretation of the structural features of $Na_2Ti_2Si_2O_9$ can be facilitated by comparing this spectrum to those of titanates with similar coordination geometries. The TiO_6 coordination geometry in $Na_2Ti_2Si_2O_9$ closely resembles that in $Na_2Ti_6O_{13}$,[37] anatase, and rutile [36] which have edge-shared TiO_6 polyhedra and three-coordinate oxygen atoms. Similar to $Na_2Ti_2Si_2O_9$, $Na_2Ti_6O_{13}$ has distorted edge-shared TiO_6 with various Ti−O bond lengths ranging from 1.82 to 2.11 Å (Table 1).[37] The octahedra share edges at one level in linear groups of three. Each group

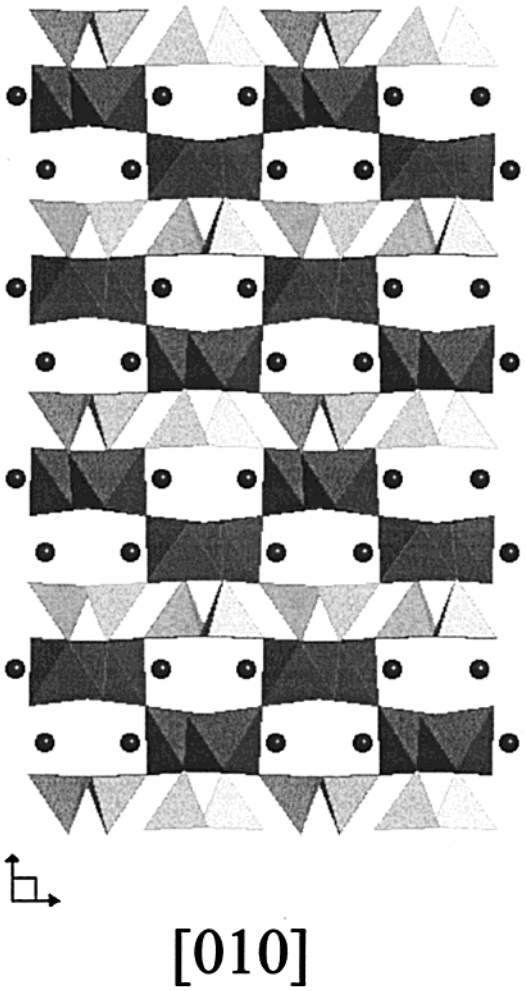

Figure 8. $Na_2Ti_2Si_2O_9$ crystal structure viewed from [010]. Ti is in edge-shared TiO_6 chains. All six Ti−O bond lengths are different, and the compound contains three-coordinate oxygens.

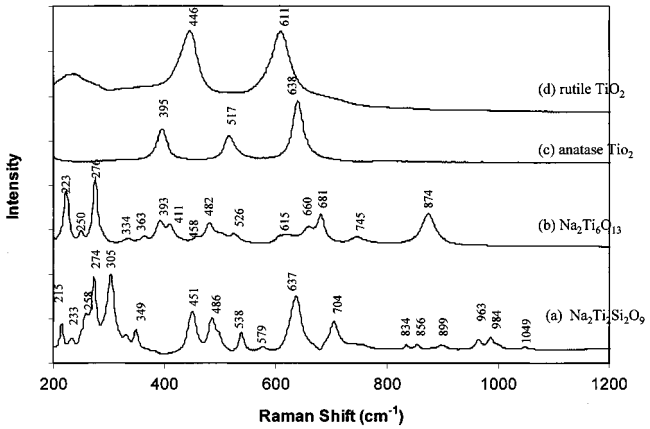

Figure 9. Raman spectra of (a) $Na_2Ti_2Si_2O_9$, (b) $Na_2Ti_6O_{13}$, (c) anatase TiO_2, and (d) rutile TiO_2.

is joined to a similar group above and below by a corner-shared apical TiO bond. These then form zigzag TiO_6 chains. The Raman spectra of $Na_2Ti_6O_{13}$, anatase, and rutile are also shown in Figure 9b−d for comparison. The major anatase Raman bands occur at 395, 517, and 638 cm^{-1}. The rutile bands occur at 446 and 611 cm^{-1}. The band around 750 cm^{-1} characteristic of the Ti−O−Ti stretch in corner-shared TiO_6 is absent in anatase and rutile as expected. Although $Na_2Ti_6O_{13}$ has edge-shared TiO_6 polyhedra and three coordinate oxygens as in anatase and rutile, it exhibits several more strong bands in the region of 400−700

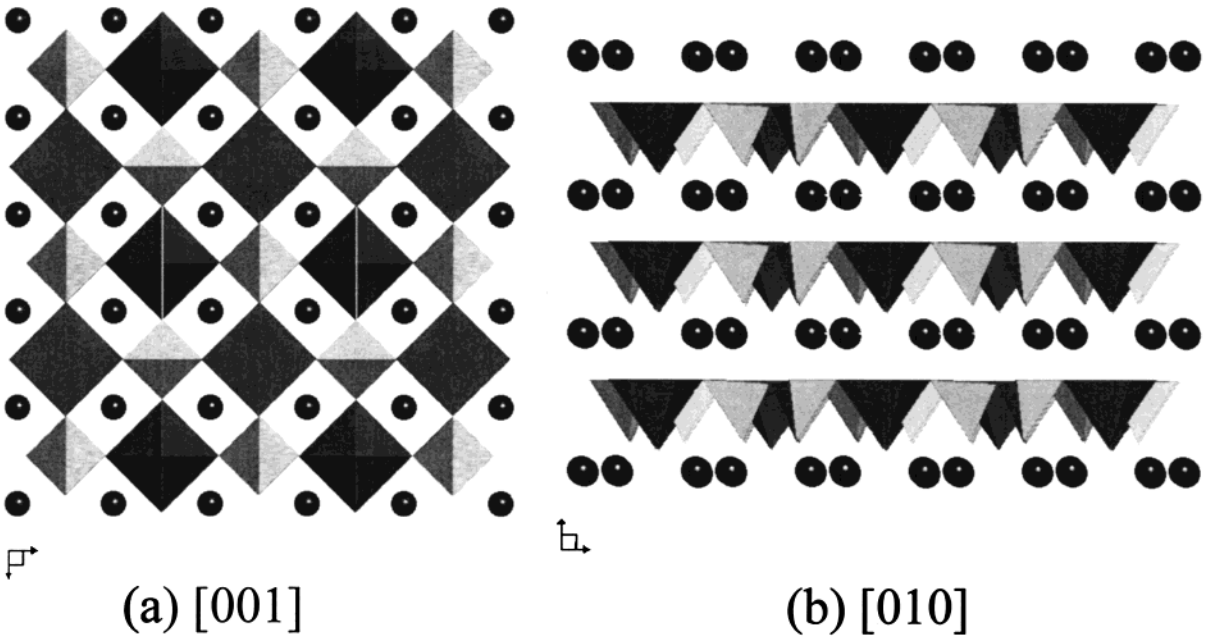

Figure 10. (a) $NaTiSiO_5$ and (b) $Ba_2TiSi_2O_8$ crystal structure viewed from [001] and [010]. Ti is in TiO_5 coordination.

cm^{-1}. $Na_2Ti_2Si_2O_9$ contains structural features similar to anatase and rutile (edge-shared TO_6); however, the structure is more similar to $Na_2Ti_6O_{13}$ which contains both edge- and corner-shared TiO_6. Therefore, different species can be distinguished from one another on the basis of pattern recognition. The peaks at 258, 274, 305, 451, 486, 538, 637, 704, 834, 856, and 899 cm^{-1} observed for $Na_2Ti_2Si_2O_9$ are similar to those seen in $Na_2Ti_6O_{13}$, which exhibits Raman bands at 223, 250, 276, 393, 411, 482, 615, 660, 681, and 874 cm^{-1}. Therefore, Raman bands at 637 and 704 cm^{-1} from $Na_2Ti_2Si_2O_9$ and 660 and 681 cm^{-1} from $Na_2Ti_6O_{13}$ are likely due to the Ti−O−Ti stretch in edge-shared TiO_6. The very weak Raman bands at 834, 854, and 897 cm^{-1} from $Na_2Ti_2Si_2O_9$ are likely due to a combination of a short Ti−O* stretch with a symmetric SiO_3 vibration, as seen in compounds with TiO_5 coordination (see Section IV). A similar Raman peak at 874 cm^{-1} is also seen in $Na_2Ti_6O_{13}$, which has a distorted TiO_6 with a short Ti−O bond. Raman bands at 963, 984, and 998 cm^{-1} from $Na_2Ti_2Si_2O_9$ are assigned to the $[O_3Si-O]^{\delta-}-[TiO_5]^{\delta+}$ stretch as discussed in Section II. The two strong bands at 274 and 304 cm^{-1} are most likely due to vibrations between sodium and oxygen bonds.

IV. Na_2TiSiO_5 (natisite), and $Ba_2TiSi_2O_8$ (fresnoite). The crystal structure of fresnoite consists of pyrosilicate $[Si_2O_7]^{6-}$ tetrahedral pairs corner-linked to TiO_5 square pyramids, with the apical oxygens of both polyhedra pointing in the same direction.[14,15] Intercalated between these sheets are Ba^{2+} ions in highly distorted pentagonal antiprisms (Figure 10b). There is a short Ti−O distance of 1.66 Å on the apical bond. The chemical composition of Na_2TiSiO_5 (natisite) is formally related to $CaTiSiO_5$ with two sodiums replacing one calcium. However, the titanium environment and crystal structure of these two compounds are very different. The structure of Na_2TiSiO_5 contains layers of SiO_4 tetrahedra and TiO_5 square pyramids joined by sharing corners and separated by layers of Na^+ ions.[12,13] Four oxygen atoms are tetragonally arranged 1.99 Å from the titanium atom and the fifth (lone) oxygen atom is only 1.695 Å from the titanium, forming a highly compressed square pyramid. Different from fresnoite, the apical oxygens of the TiO_5 square pyramids within the {001} plane point in opposite directions (Figure 10a). In the TiO_5 configurations in Na_2TiSiO_5 and $Ba_2TiSi_2O_8$, the apical oxygen is strongly bonded to titanium

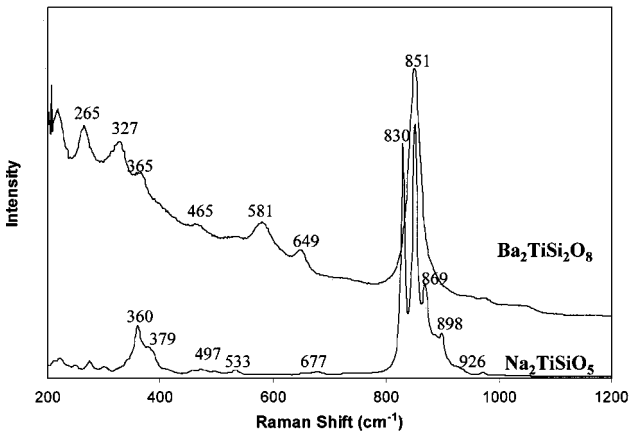

Figure 11. Raman spectra of $NaTiSiO_5$ and $Ba_2TiSi_2O_8$.

(forming what can be considered as a double Ti═O bond), and is practically not bonded to the other cations in the structure. In addition, these pyramids are isolated from the others so that the Ti−O vibrations are well-localized. High electronic density around the double bond enhances the polarizability variation when the stretching normal mode is excited. Figure 11 shows the Raman spectra of Na_2TiSiO_5 and $Ba_2TiSi_2O_8$. The most prominent bands in the spectra of both of these compounds are in the region from 800 to 900 cm^{-1}. The band positions in $Ba_2TiSi_2O_8$ are in good agreement with a powder Raman spectrum of $Ba_2TiSi_2O_8$ reported in the literature.[21−24,38] The Raman bands between 700 and 900 cm^{-1} have previously been assigned to the stretch of the shortest Ti−O* bond (O* denotes an apical oxygen), and Ti−O^- bonds (O^- denotes a nonbridging oxygen).[21−24,38] Likewise we assign the most prominent bands near ∼850 cm^{-1} for both Na_2TiSiO_5 and $Ba_2TiSi_2O_8$ to the Ti−O* stretch. However, while there is only one short Ti−O bond in both $Ba_2TiSi_2O_8$ and Na_2TiSiO_5, there is one broad strong band in $Ba_2TiSi_2O_8$, two strong bands at 858 and 873 cm^{-1} for $Ba_2TiSi_2O_8$ in previous studies),[21−24,38] and four strong bands in Na_2TiSiO_5 in the range of 800 to 900 cm^{-1}. Therefore, other vibrations contribute to the Raman spectra in this region. Through isotopic substitution of silicon and titanium, Gabelica-Robert et al. showed that the strong bands at 858 and 873 cm^{-1}

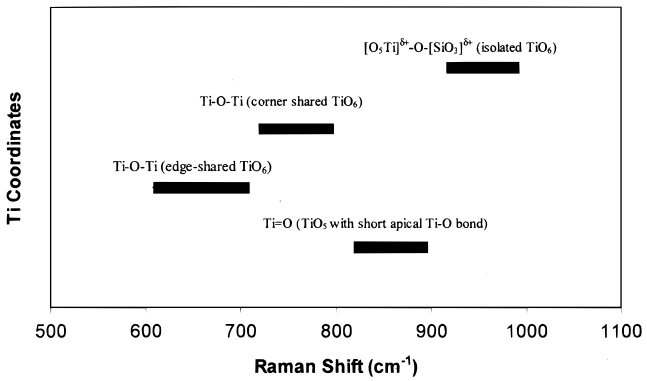

Figure 12. Correlation of Raman shifts with Ti coordination.

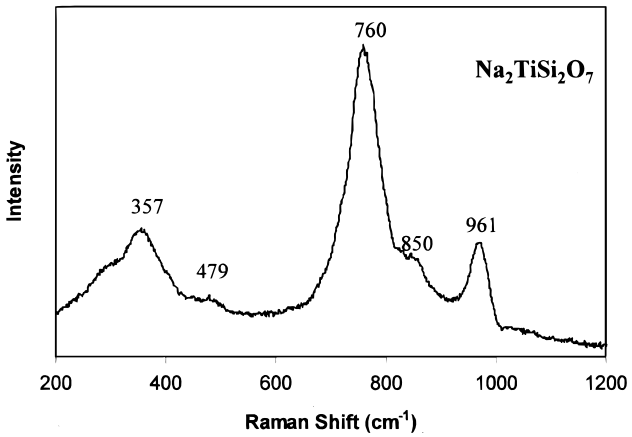

Figure 13. Raman spectrum of $Na_2TiSi_2O_7$.

in $Ba_2TiSi_2O_8$ were combinations of the short Ti−O* stretch and symmetric SiO_3 vibrational modes. The high intensity of these bands seems to support this argument. For titanate (without silicon) compounds with one short Ti−O* bond in square-pyramidal coordination, one would expect only one strong band in the region of 800 to 900 cm^{-1}. This is indeed the case for $K_2Ti_2O_5$ which contains five-coordinate titanium,[39] and has only one strong band at 898 cm^{-1}.[40]

V. Unknown Structures: $Na_2TiSi_2O_7$, ETS-4, and $CsTiSi_2O_{6.5}$. As we showed in previous sections, the relationship between Raman shifts and the local bonding configurations around silicon and titanium have been proposed and are plotted in Figure 12. For silicotitanates with regular corner-shared TiO_6 chains, a prominent band in the vicinity of "750 cm^{-1}" (700−800 cm^{-1}) is assigned to the Ti−O−Ti stretch in TiO_6 chains. For silicotitanates with TiO_6 units isolated by SiO_4 tetrahedra, a strong band at "960 cm^{-1}" (900−1000 cm^{-1}) due to $[O_3Si-O]^{\delta-}-TiO_5]^{\delta+}$ stretch will dominate in the Raman spectra. Evidence of edge-shared TiO_6 (similar to anatase and rutile) can be observed by Raman bands in the region of 600 to 700 cm^{-1}. For silicotitanates which contain TiO_5 in a square pyramidal configuration with one short T−O bond, a strong band at "850 cm^{-1}" (800−920 cm^{-1}) due to the short T═O stretch will be observed. In this section, we will use this information to help determine the structural features of unknowns: $Na_2TiSi_2O_7$, ETS-4, and $CsTiSi_2O_{6.5}$.

V.1. $Na_2TiSi_2O_7$. Although $Na_2TiSi_2O_7$ was discovered in 1979,[41] no crystal structure determination has been performed on this compound. Figure 13 shows the Raman spectrum of $Na_2TiSi_2O_7$. Since a strong band at 756 cm^{-1} was observed for $Na_2TiSi_2O_7$, similar to ETS-10 and $Na_2TiSi_4O_{11}$, we suspect that it also contains corner-shared TiO_6 chains in the framework. The broadness of this band might indicate that the Ti−O−Ti bond angle in this compound has a wider distribution than that found in the ETS-10 and $Na_2TiSi_4O_{11}$. The additional medium-strength band at 960 cm^{-1} in $Na_2TiSi_2O_7$ is assigned to a $[O_3-Si-O]^{\delta-}-[TiO_5]^{\delta+}$stretch. On the basis of composition (Figure 2) and the formal charge model,[16,17] titanium in $Na_2TiSi_2O_7$ is expected to be in octahedral coordination which is consistent with the conclusions obtained from Raman studies.

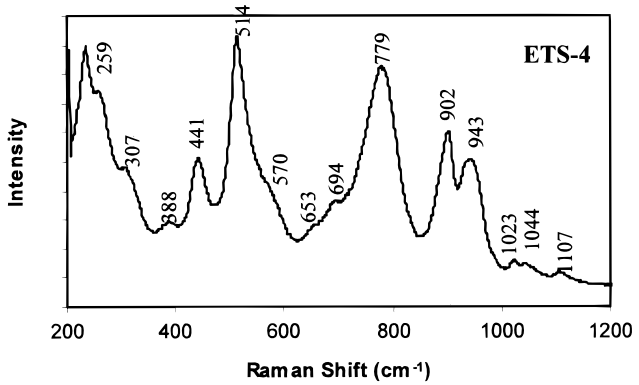

Figure 14. Raman spectrum of ETS-4.

V.2. ETS-4. ETS-4 is a microporous crystalline silicotitanate that exhibits a structure believed to be similar to zorite, $Na_6[Ti(Ti_{0.9}Nb_{0.1})_4(Si_6O_{17})_2(O,OH)_5]\bullet 11H_2O$.[42,43] The approximate chemical formula of ETS-4 is $M_6Ti_3Si_8O_{25}$, where M is sodium or potassium.[42] The ETS-4 structure proposed by Kuznicki et al.,[42] however, contains exclusively TiO_6, instead of TiO_5 and TiO_6 known in zorite. To elucidate this issue, we have obtained the Raman spectrum of ETS-4. The resulting spectrum is shown in Figure 14. The peak locations are similar to those previously reported in the literature.[44,45] However, the relative intensities are somewhat different. The strong peak at 779 cm^{-1} in ETS-4 matches the frequency we assign to compounds that contain Ti−O−Ti chains with TiO_6 coordination as proposed by Kuznicki et al. Raman bands at 903 and 943 cm^{-1} represent Ti−O−Si bonding configurations in this compound. Since there are no Raman bands around 850 cm^{-1}, TiO_5 with an apical oxygen cannot be present.

V.3. $CsTiSi_2O_{6.5}$. $CsTiSi_2O_{6.5}$ has a crystal structure isomorphous to the mineral pollucite, $CsAlSi_2O_6$, with titanium replacing aluminum.[46,47] ^{29}Si NMR, single-crystal X-ray, neutron diffraction, and X-ray absorption spectroscopy (XAS) were used to characterize this new compound $CsTiSi_2O_{6.5}$.[17,46−48] To maintain the pollucite structure and simultaneously substitute Ti^{4+} for Al^{3+}, a mechanism for charge compensation is required. Neutron and X-ray diffraction indicate that charge compensation is achieved by incorporating eight extra oxygen per unit. As a result, local distortions occur although long-range cubic symmetry is preserved.[46] However, no conclusions about the distribution of excess oxygen around titanium or silicon, or about the individual Si−O and Ti−O bond lengths, could be reached using these techniques. EXAFS and XANES studies show that $CsTiSi_2O_{6.5}$ lies in a general region where the prevalent titanium coordination is TiO_5; however, the energy shift is closer to compounds containing TiO_4.[48] ^{29}Si NMR data support a TiO_5 coordination geometry in which oxygen must be shared by two edge-sharing titanium square pyramids.[17] The Raman spectrum of $CsTiSi_2O_{6.5}$ is shown in Figure 15. On the basis of the Raman spectrum, TiO_5 with a short apical oxygen cannot be present because strong bands which are characteristic of this short apical bond are not observed in the region of 800−900 cm^{-1}. Instead, there are strong Raman bands at 645 and 717 cm^{-1} and a medium-strength shoulder band at 770 cm^{-1}. These Raman bands are most consistent with the presence of edge-shared (645

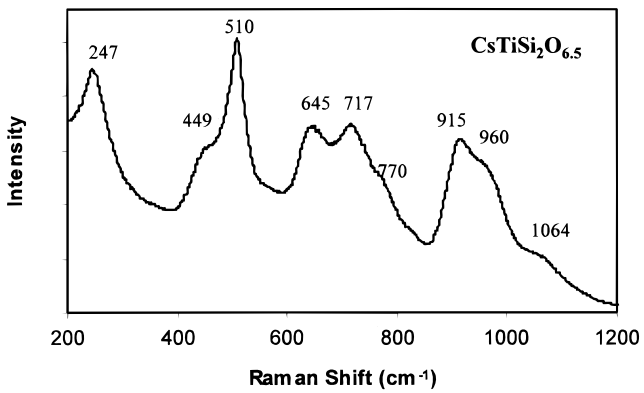

Figure 15. Raman spectrum of $CsTiSi_2O_{6.5}$.

and 717 cm^{-1}) and corner-shared (770 cm^{-1}) TiO_6 chains. Since all model compounds with TiO_5 contain short apical TiO bonds, the Raman spectra alone would lead to the conclusion that TiO_6 chains are present. However, other techniques including NMR, neutron diffraction, EXAFS, and XANES support the presence of TiO_5 in $CsTiSi_2O_{6.5}$. The reason for the discrepancy between the Raman and other techniques can be resolved by the fact that this unusual compound has edge-shared TiO_5 with no apical oxygen. Since all the Ti−O bond lengths are expected to be similar, bands due to short Ti−O bonds should not be present in the Raman spectra. A compound which contains edge-shared TiO_5 with equal Ti−O bond lengths is expected to exhibit Raman bands similar to those observed in compounds that contain edge-shared TiO_6. As discussed in Section II, the bands at 915 and 960 cm^{-1} are due to the symmetric silicon−oxygen stretching motions $[O_3Si-O]^{\delta-}-TiO_4]^{\delta+}$. The existence of these linkages is consistent with the crystal structure proposed in Balmer et al.[47] The band observed at 1064 cm^{-1} is likely due to silicate impurity in the $CsTiSi_2O_{6.5}$ sample.

The spectral features for ETS-4 are similar to those for $CsTiSi_2O_{6.5}$. For example, the peaks at 441, 514, 653, 694, 779, 902, 943, 1023, 1044, and 1107 cm^{-1} observed in ETS-4 correlate well with those seen in $CsTiSi_2O_{6.5}$, which exhibits Raman peaks at 449, 510, 645, 717, 770, 915, 960, and 1064 cm^{-1}. While ETS-4 and $CsTiSi_2O_{6.5}$ have Raman peaks at similar frequencies, however, the relative intensities of the peaks differ. The intensity of the peak assigned to Ti−O−Ti stretch in edge-shared TiO_5 is larger for $CsTiSi_2O_{6.5}$, while the intensity of the peak assigned to Ti−O−Ti stretch in a corner-shared TiO_6 is larger for ETS-4. The strong peak at 779 cm^{-1} in ETS-4 indicates the presence of Ti−O−Ti chains with TiO_6 coordination as proposed by Kuznicki et al. However, the weak bands observed at 653 and 694 cm^{-1} for ETS-4 could indicate the existence of unusual edge-shared TiO_5, as in $CsTiSi_2O_{6.5}$.

Summary

Raman spectroscopy has been used to examine the vibrational behavior and the local structures of twelve silicotitanates. The relationship between Raman shifts and the local bonding configurations around silicon and titanium have been proposed as follows. For silicotitanates with regular corner-shared TiO_6 chains, a prominent band in the vicinity of "750 cm^{-1}" (700−800 cm^{-1}) is assigned to the Ti−O−Ti stretch in TiO_6 chains. For silicotitanates with TiO_6 units isolated by SiO_4 tetrahedra, the Ti−O−Ti stretch will not be observed in the Raman spectra. Instead, a strong band at "960 cm^{-1}" (900−1000 cm^{-1}) due to $[O_3Si-O]^{\delta-}-TiO_5]^{\delta+}$ stretch will dominate in the Raman spectra. Evidence of edge-shared TiO_6 (similar to anatase and rutile) can be observed by Raman bands in the region of 600 to 700 cm^{-1}. For silicotitanates which contain TiO_5 in a square pyramidal configuration with one apical short Ti−O bond, a strong band at "850 cm^{-1}" (800−920 cm^{-1}) due to a short Ti═O stretch will be observed (see Figure 12). The results presented in this paper show that while Raman spectra can identify bonding types, Raman does not represent a "stand-alone" technique for determining structures of silicotitanates. However, when used in conjunction with other methods such as ^{29}Si NMR, the complementary information Raman spectra provides can lead to definitive structure determination.

Acknowledgment. This work was supported by the Environmental Management Science Program (EMSP). The research described in this paper was performed in part at the Environmental Molecular Sciences Laboratory, a national scientific user facility sponsored by the DOE Office of Biological and Environmental Research and located at Pacific Northwest National Laboratory (PNNL). PNNL is operated by Battelle for the U.S. Department of Energy under Contract DE-AC06-76RLO 1830.

References and Notes

(1) Anthony, R. G.; Phillip, C. V.; Dosch, R. G. *Waste Manage.* **1993**, *13*, 503.
(2) Huybrechts, D. R. C.; De Btuydker, L.; Jacobs, P. A. *Nature* **1990**, *345*, 240.
(3) Clerici, M. G.; Bellussi, G.; Romano, U. *J. Catal.* **1991**, *129*, 159.
(4) Grey, I. E.; Roth, R. S.; Balmer, M. L. *J. Solid State Chem.* **1997**, *131*, 38.
(5) Fischer, K. *Z. Kristallogr.* **1969**, *129*, 222.
(6) Anderson, M. W.; Terasaki, O.; Ohsuna, T.; Philippou, A.; MacKay, S. P.; Ferreira, A.; Rocha, J.; Lidin, S. *Nature* **1994**, *367*, 347.
(7) Pjatenko, J. A.; Pudovkina, Z. V. *Kristallografija* **1960**, *5*, 563.
(8) Zachariasen, W. H. *Z. Kristallogr.* **1930**, *73*, 7.
(9) Alexander Speer, J.; Gibbs, G. V. *Am. Miner.* **1976**, *61*, 238.
(10) Sundberg, M. R.; Lehtinen, M.; Kivekas, R. *Am. Miner.* **1987**, *72*, 173.
(11) Ch'in-hang; Simonov, M. A.; Belov, N. V. *Soviet Physics − Doklady*, **1969**, *14*, 516.
(12) Nyman, H.; O'Keefe, M. O. *Acta Crystallogr.* **1978**, *B34*, 905.
(13) Nikitin, A. V.; Ilyukhin, V. V.; Litvin, B. N.; Mel'nikov, O. K.; Belov, N. V. *Sov. Phys.-Doklady* **1965**, *9* (8), 625.
(14) Moore, P. B.; Louisnathan, J. *Science* **1967**, *156*, 1361.
(15) Masse, R.; Grenier, J.-C.; Durif, A. *Bull. Soc. Franc. Miner. Crist.* **1967**, *90*, 20.
(16) Bunker, B. C.; Balmer, M. L. *Chem. Mater*., submitted.
(17) Balmer, M. L.; Bunker, B. C.; Wang, L.; Peden, C. F. H.; Su, Y. *J. Phys. Chem. B* **1997**, *101*, 9170.
(18) Sakka, S.; Miyaji, F.; Fukumi, K. *J. Non-Cryst. Solids* **1989**, *112*, 64.
(19) Frukawa, T.; White, W. B. *Phys. Chem. Glasses* **1979**, *20*, 69.
(20) Mysen, B. O.; Ryerson, F. J.; Virgo, D. *Am. Mineral.* **1980**, *65*, 1150.
(21) Gabelica-Rober, M.; Tarte, P. *Phys. Chem. Minerals* **1981**, *7*, 26.
(22) Markgraf, S. A.; Sharma, S. K. *J. Am. Ceram. Soc.* **1992**, *75*, 2630.
(23) Markgraf, S. A.; Sharma, S. K. *J. Mater. Res.*, **1993**, *8*, 635.
(24) Stassen, S.; Tarte, P.; Rulmont, A. *Spectrochim. Acta, Part A* **1998**, *54*, 1423.
(25) Hong, S. B.; Kim, S. J. Uh, Y. S. *Korean J. Chem. Eng.* **1996**, *13*, 419.
(26) McKeown, D. A.; Bell, M. I.; Kim, C. C. *Phys. Rev. B.* **1993**, *48*, 16357.
(27) de Man, A. J. M.; Sauer, J. *J. Phys. Chem.* **1996**, *100*, 5025.
(28) Camblor, M. A.; Corma, A.; Perez-pariente, J. *J. Chem. Soc. Chem. Commun.* **1993**, 557.
(29) Deo, G.; Turek, A. M.; Wachs, I. E.; Huybrechts, D. R. C.; Jacobs, P. A. *Zeolites* **1993**, *13*, 365.
(30) Bellussi, G.; Rigutto, M. S. In *Advance Zeolite Science and Applications*; Jansen, J. C., Stocker, M., Karge, H. G., Weitkamp, J., Eds.; *Studies in Surface Science and Catalysis*; Elsevier: Amsterdam, 1994; Vol. 85, p 177.
(31) Philippou, A.; Rocha, J.; Anderson, M. W. *Catal. Lett.* **1999**, *57*, 151.
(32) Rocha, J.; Brabdao, P.; Lin, Z.; Kharlamov, A.; Anderson, M. W. *Chem. Commun.* **1996**, 669.

(33) Choisnet, J.; Deschanvres, A.; Raveau, B. *J. Solid State Chem.* **1973**, *7*, 408.
(34) Adams D. M.; Gardner, I. R. *J. Chem. Soc., Dalton Trans*. **1976**, 315.
(35) McMillan, P. *Am. Miner*. **1988**, *69*, 622.
(36) Palmer, D. *Crystal Maker, Interactive Cxrystallography for MacOS*; Oxfodshire, OX6 7BS, U.K.
(37) Andersson, S.; Wadsley, A. D. *Acta Crystallogr*. **1962**, *15*, 194.
(38) Blasse, G. *J. Inorg. Nucl. Chem.* **1979**, *41*, 639.
(39) Andersson, S.; Wadsley, A. D. *Acta Crystallogr*. **1961**, *14*, 1245.
(40) Bamberger, C. E.; Begun, G. M.; MacDougal, C. S. *Appl. Spectrosc.* **1990**, *44*, 30.
(41) Glasser, F. P.; Marr, J. *J. Am. Ceram. Soc*. **1979**, *62*, 42.
(42) Kuznicki, S. M.; Thrush, K. A.; Allen, F. M.; Levine, S. M.; Hamil, M. M.; Hayhurst, D. T.; Mansour, M. Synthesis and Adsorptive Properties of Titanium Silicate Molecular Sieves. In *Synthesis of Microporous Materials*, Vol. 1—Molecular Sieves; Ocelli, M. L., Ed.; Van Nostrand Reinhold: New York, 1992; p 427.
(43) Sandomirskij, P. A.; Belov, N. V. *Sov. Phys. Crystallogr.* **1979,** *24*, 686.
(44) Valtchev, V.; Mintova, S.; Mihailova, B.; Konstantinov, L. *Mater. Res. Bull.* **1996**, *31*, 163.
(45) Mihailova, B.; Valtchev, V.; Mintova, S.; Konstantinov, L. *Zeolites* **1996**, *16*, 22.
(46) McCready, D. E.; Balmer, M. L.; Keefer, K. D. *Powder Diffr*. **1997,** *12*, 1.
(47) Balmer, M. L.; Huang, Q.; Wong-Ng, W.; Roth, R. S.; Santoro, A. *J. Solid State Chem.* **1997**, *130*, 97.
(48) Hess, N. J.; Balmer, M. L.; Bunker, B. C.; Conradson, S. D. *J. Solid State Chem.* **1997**, *129*, 206.